

Behavior of Hydraulic Machinery under Steady Oscillatory Conditions  
- Researches in Japan -

Hideo OHASHI\* and Hiroshi MIYASHIRO\*\*

Introduction

This paper presents the state-of-the-art in Japan on the research on the behavior of hydraulic machinery under steady oscillatory conditions.

Papers written by the Japanese are divided into the following topics, listed and summarized.

(a) Oscillatory behavior of the turbomachinery and their transfer functions

Many papers deal with the response of the turbomachinery to the oscillatory flow. Fundamental studies are included.

(b) Pressure fluctuation in pump pipeline

Two papers describe a resonator, a branch pipe of a quarter wave length, and the pipe length equivalent to the pump, respectively.

(c) Stability of hydraulic machinery systems

This topic is divided into two categories. One is the instability caused by cavitation. Another is the oscillatory behavior of vortex core in draft tubes of hydraulic turbines.

(d) Links with hydro-elastic phenomena in the machine and in the system

Most papers deal with fluid force, which acts on pump impellers and turbine runners and may cause hydro-elastic vibrations.

---

\* Professor, The University of Tokyo, Tokyo, Japan.

\*\* Chief Researcher, Mechanical Engineering Research Laboratory, Hitachi, Ltd., Tsuchiura, Japan.

(a) Oscillatory behavior of the turbomachinery  
and their transfer functions

List of Papers

- (a1) Ohashi, H., "Dynamic Characteristics of Turbopumps. 1st Rep. Pressure Rise Response of Linear Cascade to Fluctuating Flow Rate", Trans. JSME, Vol. 33, No. 255, Nov. 1967, pp. 1769-1778, (in Japanese).
- (a2) Ohashi, H., "Dynamic Characteristics of Turbopumps. 2nd Rep. Theoretical Study", Trans. JSME, Vol. 33, No. 255, Nov. 1967, pp. 1779-1788, (in Japanese).
- (a3) Ohashi, H., "Dynamic Characteristics of Turbopumps. 3rd Rep. Experimental Study", Trans. JSME, Vol. 33, No. 255, Nov. 1967, pp. 1789-1799, (in Japanese).
- (a1) to (a3) are equivalent to "Analytical and Experimental Study of Dynamic Characteristics of Turbopumps", NASA Technical Note TN D-4298, April 1968, by the same author.
- (a4) Shoji, H., Ohashi, H. and Kemp, N.H., "Forces on Staggered Airfoil Cascades in Unsteady In-Phase Motion", J. Fluids Eng., Vol. 103, No.2, June 1981, pp. 299-306.
- (a5) Shimura, T. and Kamijo, K., "Dynamic Response of a Centrifugal Liquid Oxygen Rocket Pump", ASME Paper 83-FE-24, Fluids Engineering Conference, June 1983, Houston.
- (a6) Nishiyama, T. and Nishiyama, H., "Dynamic Transfer Characteristics of Partially Cavitated Hydrofoil Cascades in Translatory Gust (Cavitation Compliance and Mass Flow Gain Factor)", Trans. JSME, Vol. 47, No. 415, March 1981, pp. 412-422, (in Japanese).
- (a7) Nishiyama, T. and Nishiyama, H., "Dynamic Transfer Characteristics of Partially Cavitated Hydrofoil Cascade (Compressibility Effects in Gaseous Liquid Flow)", Trans. JSME, Vol. 47. No. 418, June 1981, pp. 924-935, (in Japanese).

Summary

Papers a1 to a3 deal with the response of pressure rise of a turbopump to fluctuating flow rate. The problem is however restricted to incompressible case, that is, to non-cavitating pumps. The result can also be applied to fans and blowers, as far as the flow can be assumed incompressible.

The response of pressure rise bases on the dynamic behavior of cascade to unsteady inlet flow. In a1 unsteady inlet condition associated with fluctuating flow rate was discussed, and it concluded that cascade behavior to in-phase translatory and sinusoidal gust should be known. Whitehead, D.S. solved this problem already in 1960 for the most general case, that is, compressible unsteady flow through linear cascade for translatory and sinusoidal inlet gust with an arbitrary phase difference. Whitehead's solution is however numerical. To the contrary paper a2 bases on an analytical solution for unstaggered linear cascade. Paper a4 expanded the latter analysis to staggered cascade, and described unsteady forces on cascade airfoil in terms of quasi-steady, apparent-mass and wake-effect lift, as usually classified for an isolated unsteady airfoil.

When flow rate is steady, the pressure difference between delivery and suction port of a pump,  $p_d - p_s$ , is totally caused by the pressure rise ability of the impeller. In the case of fluctuating flow rate, however, a part of the pressure difference is merely caused by the inertia effect of conduit, and the real pressure rise through impeller is

$$\text{pressure rise} = (p_d - p_s) + \rho L_{eq} d(Q/A)/dt \quad (a1)$$

where  $L_{eq}$  is equivalent length of the pump,  $Q$  is flow rate,  $A$  is reference cross section area.

In paper a3, a single stage centrifugal pump was used for unsteady experiment and the amplitude and phase relation of dynamic pressure rise to quasi-steady one was evaluated for a wide frequency range.

Fig.a1(a) and (b) show amplitude gain (dB) and phase shift (deg.) in dependence of reduced frequency  $\omega_R$ ,

$$\omega_R = \cos \lambda_R f / N \varphi n \quad (a2)$$

where  $\lambda_R$  is stagger angle of impeller cascade,  $N$  is number of impeller blades,  $\varphi$  is flow coefficient,  $f$  is fluctuation frequency and  $n$  is rotational frequency. In Fig.a1, analytical response by a simplified model described in paper a2 is also plotted besides measured data.

From the result of Fig.a1 followings can be concluded.

1) There is a critical reduced frequency, below which quasi-steady assumption is acceptable. From the experiment and analysis, critical reduced frequency is around 0.1 .

For a typical impeller with  $\lambda_R = 25$  deg.,  $N=8$  and  $\varphi=0.1$ , critical frequency  $f_{cr}$  is calculated from eq.(a2) as

$$f_{cr} \cong 0.1 n \quad (a3)$$

Critical frequency lies in the magnitude around one tenth of the rotational frequency.

2) Beyond reduced frequency, the dynamic response of pressure rise deviates remarkably from the quasi-steady one and the response can be roughly approximated by the first order lag, represented by the transfer function of  $1/(1+Ts)$  where time constant  $T = 1/2\pi f_{cr}$ .

Therefore, transfer matrix of non-cavitating pump can be approximated by;

$$\begin{aligned} Z_{11} &= Z_{21} = Z_{22} = 0 \\ Z_{12} &= Rp/(1+Ts) - (\rho L_{eq}/A) s \end{aligned} \quad (a4)$$

In the above mentioned study, the author tried to separate dynamic pressure rise by impeller action from pressure difference due to inertia using eq.(a1). This requires to assume a proper equivalent length  $L_{eq}$ . It is impossible, however, to determine  $L_{eq}$  by experiment in an exact sense and this implies that some guess work cannot be expelled in this process. Since the critical frequency of non-cavitating pump is fairly high, a slight error in the assesment of  $L_{eq}$  results in an amplified misevaluation of impeller pressure rise. This is an inherent weakness of this methodology.

Paper a5 reports measured response of a centrifugal liquid oxygen rocket pump. The test was done in National Aerospace Laboratory with liquid nitrogen as working fluid. The flow rate was forced to fluctuate by perturbation valve installed at delivery line. The impeller was equipped with a cavitating inducer and the emphasis of the study was laid on the determination of  $Z_{11}$  and  $Z_{12}$  components.

The result showed expected tendency. Within frequency range up to 40 Hz, measured  $Z_{12}$  agreed with quasi-steady assumption.

Papers a6 and a7 by Nishiyamas deal with dynamic response of linear cascade with partially developed cavities. This problem was solved by Brennen and Acosta (Trans. ASME, Ser. I, Vol. 98, No. 2, 1976), but under the assumptions;

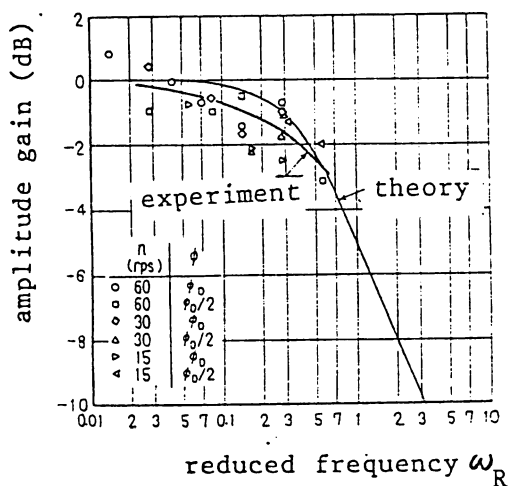
- 1) Closure model was used at the cavity end, leading to an unnecessary restriction to the change of cavity volume.
- 2) Semi-infinite chord length was assumed, neglecting unsteady effect from the flow downstream of trailing edge.

Paper a6 introduced semi-closure model at the cavity end, whose width changed in accordance with the conservation of mass and momentum, and adopted finite chord length. The response of pressure rise to fluctuating flow rate, cavitation compliance and mass flow gain factor were calculated for various cavity length and reduced frequency, and were compared with those of Brennen and Acosta. The difference is especially evident in the calculated phase angle as shown in Fig.a2, where lead (Nishiyama) and lag (Brennen) tendency is quite opposite.

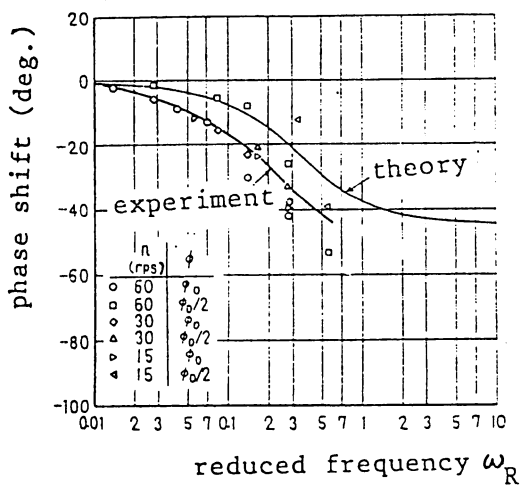
Paper a7 deals with the same problem, but introduces further compressibility of the flow outside of cavities into consideration. The flow was assumed to be homogeneous and isentropic. Fig.a3 shows the result how pressure rise (averaged over a spacing) through a linear cascade changes with void fraction  $\theta$  and reduced frequency  $k$ , where the result by Brennen and Acosta is also plotted for comparison.

In the field of unsteady cascade flow, analyses have advanced far beyond the level which can be proved by proper experimental method. More experimental studies are expected in the coming years.

Figures



(a) amplitude



(b) phase

Fig.a1 Response of pressure rise of a non-cavitating centrifugal pump

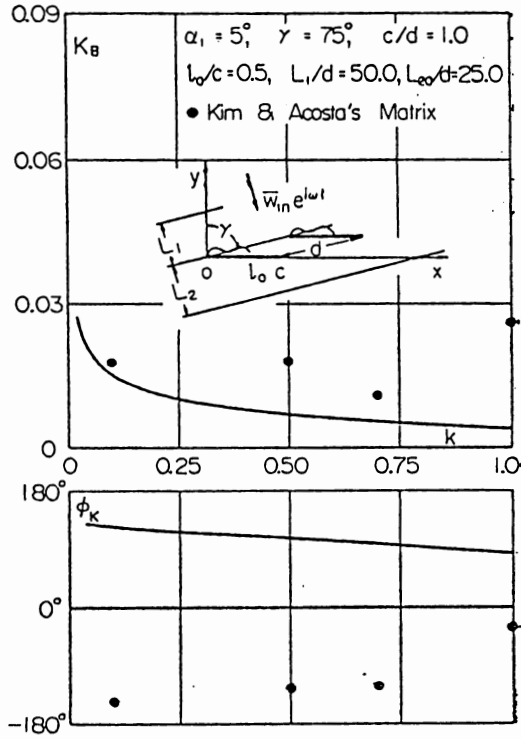


Fig.a2 Cavitation compliance of partially cavitating cascade

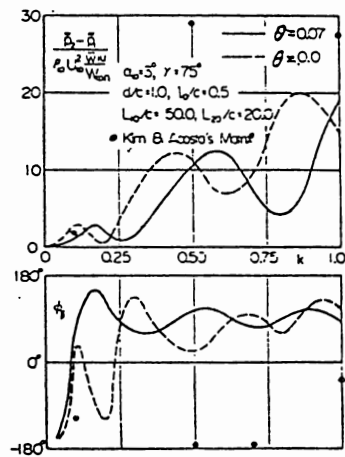


Fig.a3 Response of pressure rise of cavitating cascade without void and with void fraction of 0.07

(b) Pressure fluctuation in pump pipeline

List of Papers

- (b1) Kondo, M., Sudo, S. and Yamada, S., "Pressure Fluctuation in Pump Pipeline", Proc. IAHR Congress, Baden Baden, Vol. 5, 1977, pp. 201-206.
- (b2) Sano, M., "A Study of Pressure Fluctuation in Turbopump Pipeline System. 1st Rep. Experiments on Natural Frequency of Pipeline of Centrifugal Pumps", Trans. JSME, Vol. 49, No. 440, 1983, pp. 828-836, (in Japanese).

Summary

Paper b1 deals with the pressure fluctuation caused by pump impeller vanes. The pressure fluctuation has the frequency of  $n \times z$ , and propagates in the discharge pipeline, where  $n$  is pump speed rps and  $z$  is number of the vanes.

The distribution of the pressure fluctuation was calculated along the discharge pipeline shown in Fig.b1. Effects of a  $1/4$  wavelength branch pipe and a damper pipe with rubber wall were examined. Measurements agree well with the calculation, as shown in Fig.b2.

In paper b2, the distribution of pressure fluctuations along the suction and discharge pipes of a double suction volute pump were measured. Figure b3 shows the influence of the length  $l_s$  of the suction pipe on the pressure distribution, where  $l_s^*$  is  $l_s/d_s$  (diameter of suction pipe). Equivalent length of the pump was obtained by using a test arrangement, where the test pump was standstill.

Figures

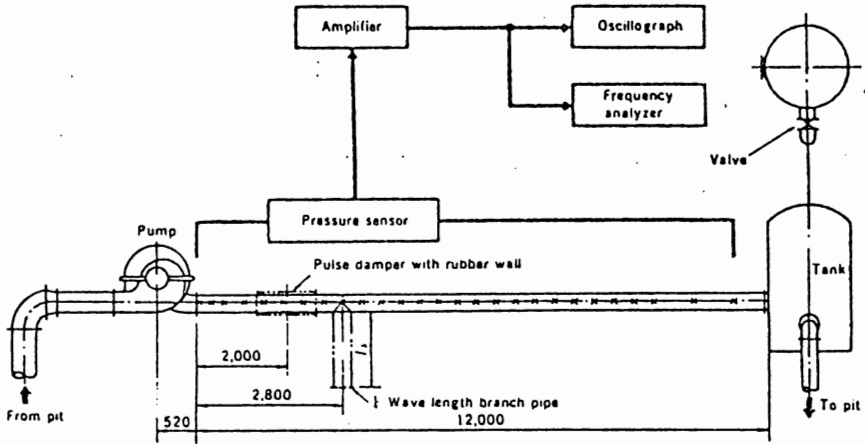


Fig.b1 Experimental apparatus and measuring instruments

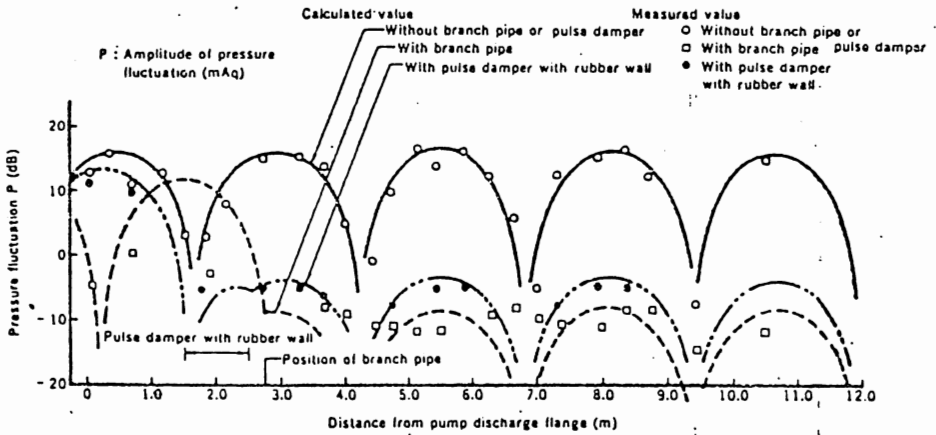


Fig.b2 Test results for a simple pipeline

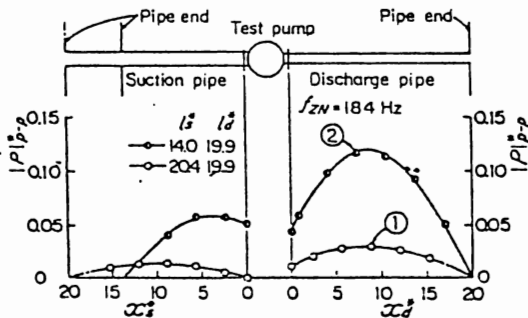


Fig.b3 Standing wave in suction and discharge pipes (Influence of length of suction pipe on pressure distribution)



(c) Stability of hydraulic machinery systems

List of Papers

- (c1) Kaneko, M. and Ohashi, H., "Self-Excited Oscillation of a Centrifugal Pump System under Air/Water Two-Phase Flow Condition", Proc. IAHR Symposium, Amsterdam, Vol. 2, 1982, Paper 36, pp. 14.
- (c2) Watanabe, T. and Kawata, Y., "Research on the Oscillation in Cavitating Inducer", Proc. IAHR Symposium, Fort Collins, Vol. 2, 1978, pp. 265-277.
- (c3) Kamiyo, K., Shimura, T. and Watanabe, M., "An Experimental Investigation of Cavitation Inducer Instability", ASME Paper 77-WA/FE-14, 1977, pp. 12.
- (c4) Shimura, T. and Kamiyo, K., "Dynamic Characteristics of Liquid Oxygen Pumps", Cavitation and Multiphase Flow Forum, ASME, 1983, pp. 39-42.
- (c5) Kitamura, N. and Kubota, N., "Cavitation Performance of Tandem Impeller at Partial Capacities", Proc. IAHR Symposium, Fort Collins, Vol. 2, 1978, pp. 621-630.
- (c6) Yamamoto, K., "An Experimental Study on Instability in a Cavitating Centrifugal Pump with a Volute Suction Nozzle", Proc. IAHR Symposium, Tokyo, Vol. 1, 1980, pp. 303-312.
- (c7) Kubota, N. and Asami, Y., "Unstable Characteristics of Mixed Flow Pumps", JSME, Preprint 800-14, 1980, pp. 297-299, (in Japanese).
- (c8) Yamabe, M., "Hysteresis Characteristics of Francis Pump-Turbines When Operated as Turbine", Trans. ASME, J. Basic Eng., Vol. 93, No. 1, 1971, pp. 80-84.
- (c9) Yamabe, M., "Improvement of Hysteresis Characteristics of Francis Pump-Turbines When Operated as Turbine", Trans. ASME, J. Basic Eng., Vol. 94, No. 3, 1972, pp. 581-585.
- (c10) Yamabe, M., "Occurrence Mechanism of Turbine Hysteresis Phenomenon of Francis-Type Pump-Turbine", ASME Paper 78-WA/FE-17, 1978, pp. 8.
- (c11) Hosoi, Y., "Contributions to Model Tests of Draft Tube Surges of Francis Turbines", Proc. IAHR Symposium, Fort Collins, Vol. 1, 1978, pp. 141-150.
- (c12) Nishi, M., et al., "Study on Swirl Flow and Surge in an Elbow Type Draft Tube", Proc. IAHR Symposium, Tokyo, Vol. 1, 1980, pp. 557-568.

- (c13)Nishi, M., et al., "Flow Regimes in an Elbow-Type Draft Tube, Proc. IAHR Symposium, Amsterdam, Vol. 2, 1982, Paper 38, pp. 13.
- (c14)Nagafuji, T. and Takigawa, H., "Characteristics of Pressure Fluctuations in Francis Turbines", Turbomachinery Society of Japan, Conf. Preprint, 1983, pp. 43-49, (in Japanese).

### Summary

A severe low-frequency oscillation was observed in a system of a pump operated in air/water two-phase flow. Paper c1 deals with this oscillation, which is different from the surging caused by the system instability. A series of experiments was carried out to find the cause of the oscillation.

The oscillation occurs under the following condition: Air is supplied to the suction pipe at proper distance upstream of the pump, and the pressure difference between the supplied air and the suction pipe is small.

Figure c1 shows time histories of the following dimensionless quantities: Air quantities  $\beta_1$  at the air supply point and  $\beta_s$  at the pump suction port, flow rate  $\phi_e$  and pump head  $\psi_e$ . The measurements reveal that the oscillation is caused by the instability concerned with the delay time, in which air bubbles are transported from the supply point to the suction port: Air bubbles reach the suction port, pump head  $\psi_e$  drops rapidly and flow rate  $\phi_e$  decreases, the pressure difference at the air supply point decreases, and  $\beta_1$  becomes zero. When the suction condition returns to single-phase, the pump recovers its head, flushing away air bubbles from its impeller. This phenomenon is repeated.

Stability criteria of the system was obtained by an analysis, using a simplified model shown in Fig. c2. A numerical analysis was made to calculate the time histories of relevant quantities, limit cycle and oscillation period.

Papers c2 to c4 treat the oscillation in cavitating inducers.

In paper c2, cavitation in a helical inducer was precisely observed. The observation revealed that the back flow at the suction of the inducer in partial flow range had a great influence on low-frequency oscillation.

A new cavitation model, i.e. the total cavitation volume consisted of the vane cavity and also the back flow one shown in Fig. c3, was

presented to calculate the compliance  $C_p$  and the mass flow gain factor  $M_B$  by using transfer matrix.

A linearized analysis of stability of the pump system was carried out. A result is shown in Fig. c4, where  $m$  is flow ratio and  $\mu$  is inclination of cavitation characteristic curve of the inducer.

Paper c3 describes measurements of dynamic pressure and observation of cavitation phenomena. The difference between the rotating cavitation and cavitation which induced low-cycle pressure oscillations was examined. The low-cycle oscillations occurred in the region where the inclination of the suction performance curves shown in Fig. c5 was negative. An example of the measurements is shown in Fig. c6.

Paper c4 describes a series of experiments, which was carried out to examine dynamic characteristics of liquid oxygen centrifugal pumps with an inducer. The experiment was made by using water, liquid nitrogen and liquid oxygen. Effects of inducer tip clearance on the low-cycle pressure oscillation were examined. In case of greater tip clearance, the back flow at the inducer inlet was greater, and the low-cycle oscillation shown in Fig. c7 occurred.

Papers c5 to c7 deal with instability caused by cavitation in centrifugal pumps.

Paper c5 treats the cavitation performance and the flow pattern in a tandem impeller, which consists of a mixed flow type inducer and a centrifugal impeller. Experiments were carried out at low flow rates, especially when a back flow occurred.

Figure c8 shows that the flow pattern in the suction approach is classified into three different types by cavitation coefficient  $K$  at low flow rates  $\phi < \phi_c$ , where  $K$  is  $NPSH/(u_t^2/g)$  and  $u_t$  peripheral velocity of the main impeller, flow coefficient  $\phi$  and head coefficient  $\psi$  are  $Q/(Au_t)$  and  $gH/u_t^2$  respectively. At zone A, the back flow was observed at large radii in the suction approach, but fluctuation of the flow was limited. At zone C, no back flow and no fluctuation were observed. At zone B, the flow pattern was complex, and the back flow and the normal one occurred alternately. Considerable fluctuation of the flow occurred as well.

Paper c6 describes a series of cavitation tests, which was carried out on a centrifugal pump with a suction volute casing. Cavitation characteristic curves are shown in Fig. c9, where  $K_d$  is  $2(p_1 - p_v)/(\rho w_1^2)$ . Weak oscillation caused by rotating cavitation and heavy oscillation

of low frequency occurred. Frequency of the heavy oscillation was generally independent of the suction pipe length. There was a region of NPSH, where the frequency of the oscillation changed discontinuously. In this region both rotating cavitation and system oscillation, the heavy oscillation, were observed. This is caused by the following reason: The back flow accompanied by cavitation rotates in the suction volute casing, does not go upstream into the suction pipe, and is mixed up with the incoming flow at the impeller inlet.

Paper c7 describes a series of experiments, which was carried out on unstable characteristics of a mixed flow pump at low flow rates. Influence of number of impeller vanes  $z$  on the characteristics is shown in Fig. c10. Zones A, B and C denote the back flow region, the transition region from back flow to normal one, and the normal flow region, respectively, as described in paper c5.

Low-frequency pressure oscillation occurred in case of  $z = 6$ , but did not in case of  $z = 3$ . The oscillation is caused by periodic change in flow patterns at the impeller inlet. The back flow at the impeller inlet causes a vortex between the neighboring vanes, as shown in Fig. c11. Cavitation induced by the vortex changes the flow pattern. In case of smaller solidity, i.e.  $(l/t)_{\text{tip}} < 0.91$ , the oscillation does not occur, since the wide flow passage is not reduced by the above mentioned cavitation.

Papers c8 to c10 deal with hysteresis characteristics of turbine operation of Francis pump-turbines.

In paper c8 the hysteresis characteristics of two pump-turbine models were measured. Some results are shown in Fig. c12. Observed behavior of cavitation is different each other at two corresponding points on a hysteresis curve, as shown in Fig. c13.

Paper c9 describes experiments, which were carried out to prevent the hysteresis characteristics from occurring. Low efficiency point b is caused by reverse flow on surface I shown in Fig. c14.

Concept of swept-back wing was applied to improve velocity distribution on surface I, as shown in Fig. c15. Figure c16 shows that the swept-back leading edge of the runner vanes eliminates the hysteresis loop.

The mechanism of the hysteresis characteristics was further investigated in paper c10. The following observations clarified the cause of the reverse flow: Observation of oil film patterns on runner passage

surfaces and observation of flow near the passage entrance and outlet by using tufts.

When the twist of runner vanes begins to increase suddenly at some distance from the leading edge of the vane, secondary flow originated near this point causes reverse flow near the corner of the vane pressure surface and the crown. Then flow separation occurs at the corner, spreads, and causes the hysteresis characteristics. Small baffle, which was attached at the above mentioned corner at 10 to 30 percent distance from the vane leading edge, was effective against the hysteresis.

Papers c11 to c14 treat the draft tube surge of hydraulic turbines under partial load conditions.

Paper c11 deals with the similarity of pressure fluctuations of the surge between a model and a prototype. The prototype is Francis type, and its specific speed is 105.5 in units of m and kW.

Experimental results of the model were compared with the field test data of the prototype. Both data are in good agreement as shown in Fig. c17, where  $\Psi$  is dimensionless amplitude defined as  $\Delta h/H$  and  $\mu$  is dimensionless frequency  $f/n$ (rps). Measurements at several pressure taps, for instance taps 1 and 2 in Fig. c17, revealed that there were several types of the pressure fluctuations, for instance synchronous fluctuations, which were often severe, and asynchronous ones with circumferential phase difference.

In papers c12 and c13 the swirl flow in draft tube was induced by a set of guide vanes instead of a turbine runner.

Measurements of pressure pulsation and observation of vortex core were made in paper c12. Figure c18 shows a comparison of surge characteristics in this experiment with those in a model turbine, where  $K$  is cavitation parameter  $(H_a - H'_s - H_v)/(\bar{u}_i^2/2g)$ ,  $\bar{u}_i$  mean velocity at the draft tube inlet,  $\Delta\Psi$  is dimensionless pressure  $\Delta h/(\bar{u}_i^2/2g)$ ,  $S_t$  frequency parameter  $fD/\bar{u}_i^2$ ,  $D$  diameter of draft tube,  $m$  swirl rate  $R_i \tan\alpha/(2B)$ ,  $R_i$  radius at draft tube inlet,  $\alpha$  radial inclination of flow through guide vanes,  $B$  span of a guide vane.

Paper c13 describes the velocity distribution of the swirl flow and the behavior of the flow.

The velocity distribution was calculated on the assumption that the main flow outside the dead water region was irrotational. The behavior of the flow has four types shown in Fig. c19. Pressure fluctuations at points 1, 2, 3, 4 and 5 in Fig. c19 are shown in Fig. c20. A method of

predicting the surge frequency was proposed.

In paper c14, influence of the solidity  $l/t$  of runner vanes on the pressure fluctuation was studied experimentally, using a model of a Francis turbine of the specific speed of 240 in units of m and kW.

Large solidity induced strong vortex core which caused large pressure fluctuation. In case of small solidity, vortex core was irregular and it caused flow separation and noise at the vane inlet. Small quantity of air injected upstream of the runner was effective in noise reduction. An adequate value of the solidity must be selected.

Figures

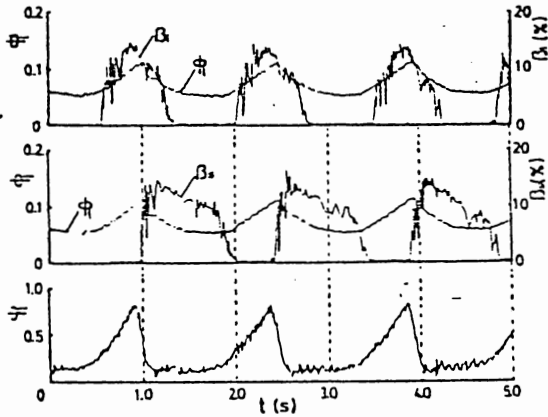


Fig.c1 Time histories of  $\phi_L$ ,  $\psi_L$ ,  $\beta_1$  and  $\beta_s$

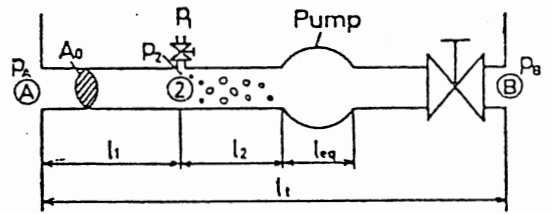


Fig.c2 Simplified model of the pumping system

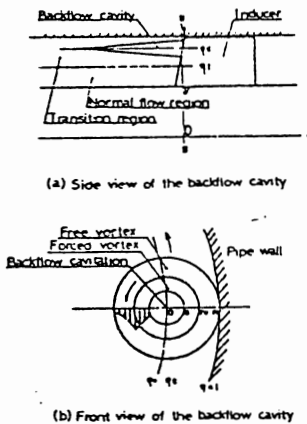


Fig.c3 Back flow cavitation model

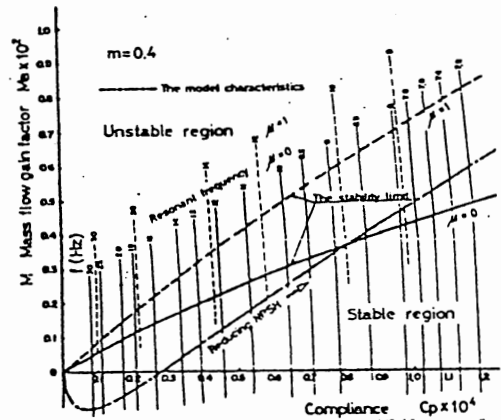


Fig.c4 Relation between system resonant frequency and  $C_p$ ,  $M_B$

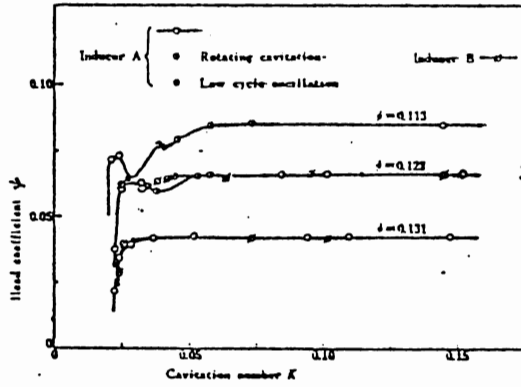
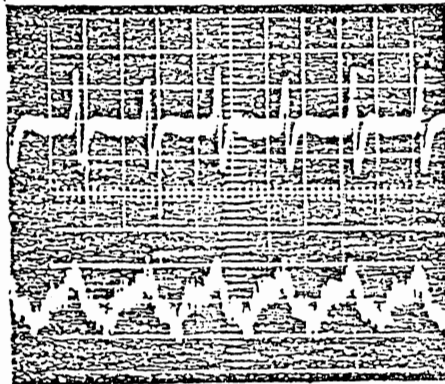


Fig.c5 Suction performance of test inducers



Inlet:  
0.36 ata/div.

Outlet:  
0.99ata/div.

50 ms/div.

$N=7,500$  RPM,  $K=0.026$ ,  $\varphi=0.104$

Fig.c6 Low-cycle pressure oscillation induced by cavitation

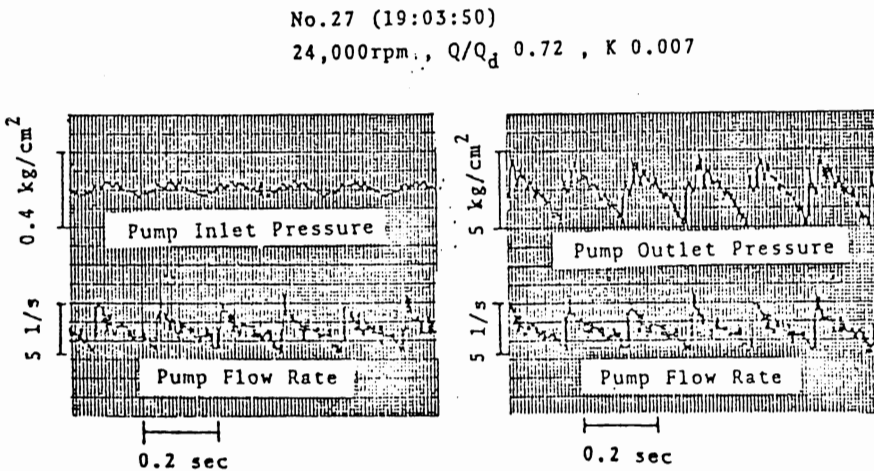


Fig.c7 Wave shape of low-cycle oscillation

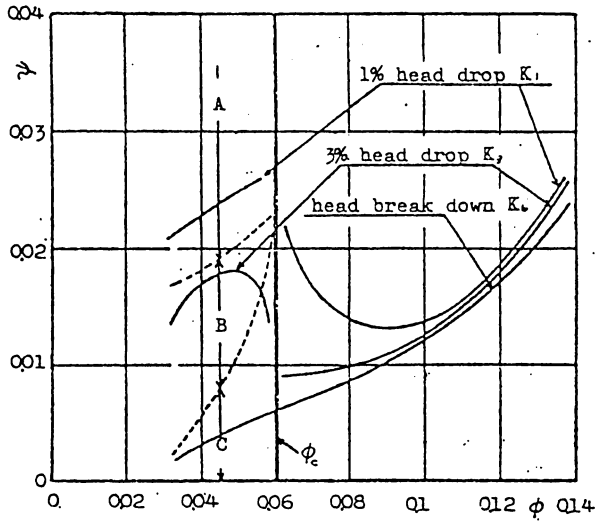


Fig.c8 Cavitation performance and flow fluctuation

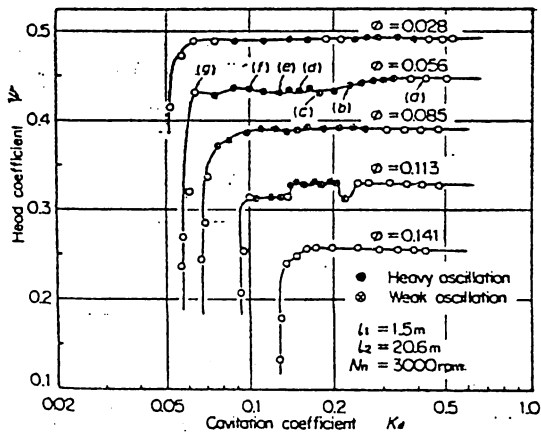


Fig.c9 Cavitation characteristic curves

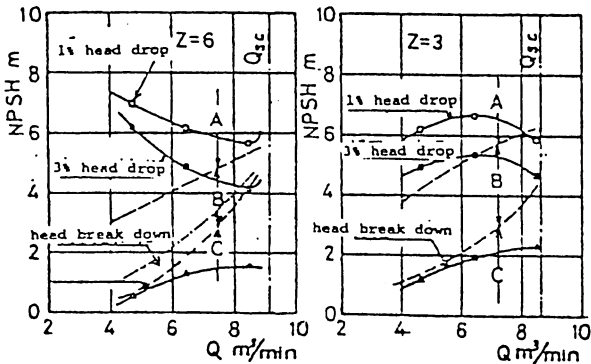


Fig.c10 Influence of number of vanes on cavitation performance



Fig.c11 Cavitation at low flow rates



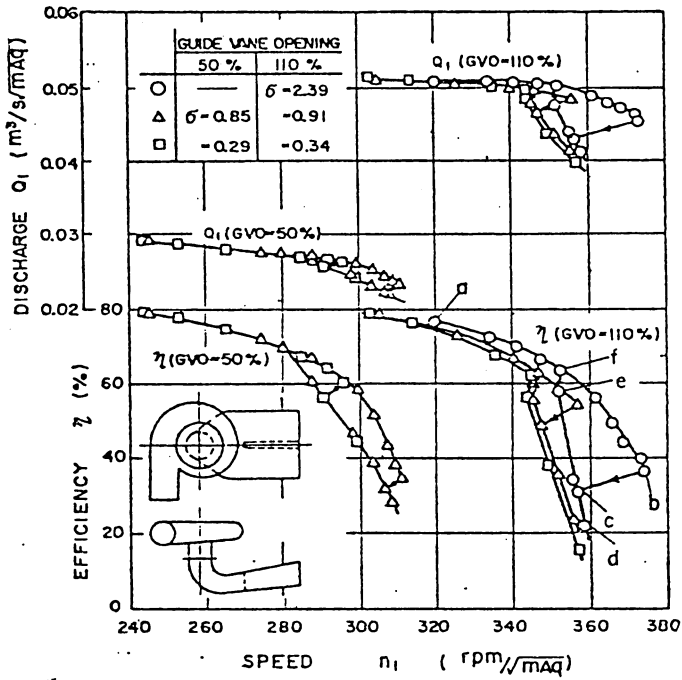


Fig.c12 Hysteresis characteristics of model pump-turbine (A)

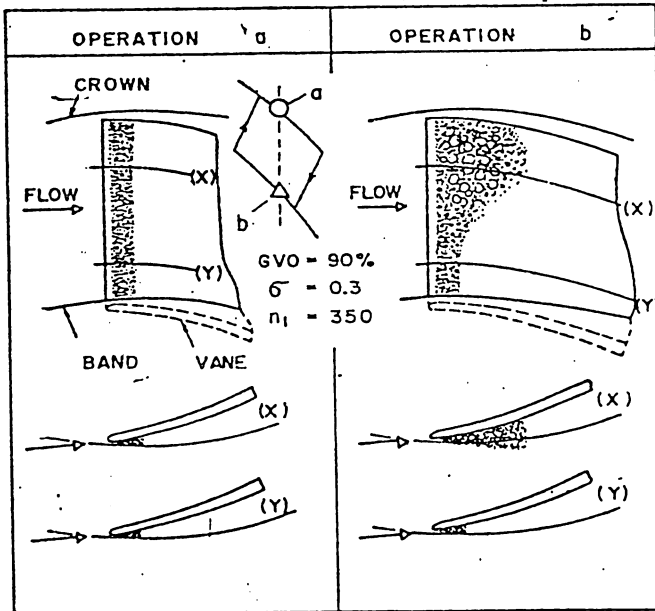


Fig.c13 State of cavitation at the entrance of runner vanes of model pump-turbine (A')

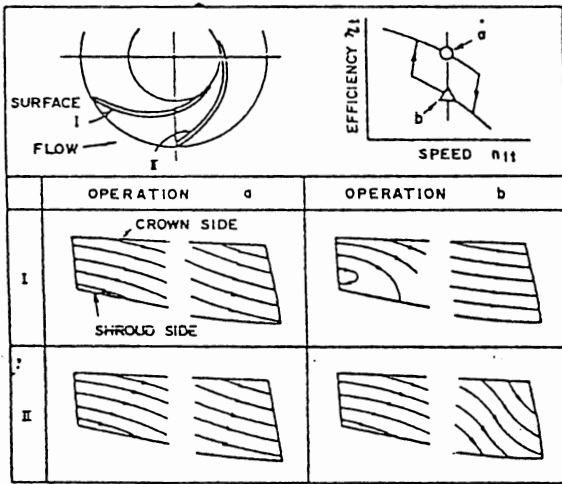


Fig.c14 Hysteresis characteristics of turbine and oil film patterns on the surface of runner vane: Pump-turbine (A-0)

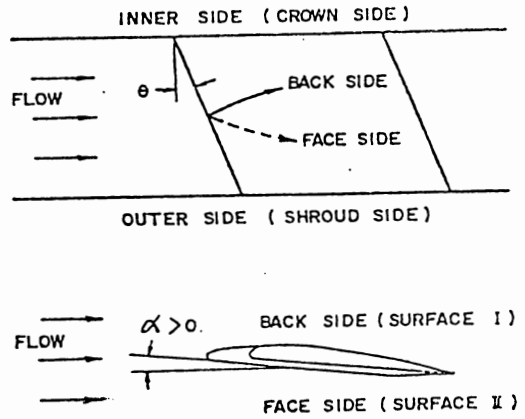


Fig.c15 Flow deflection characteristics of sweepback

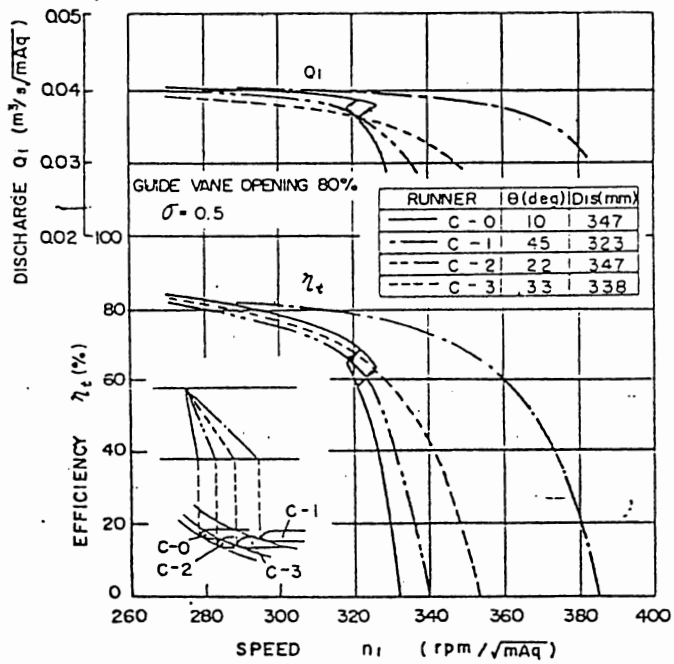


Fig.c16 Entrance shape of runner vanes and turbine performance: Pump-turbine (C)

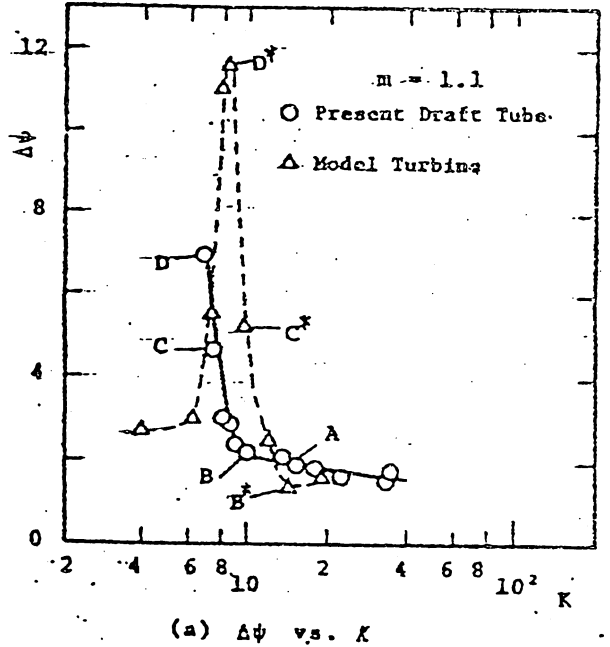
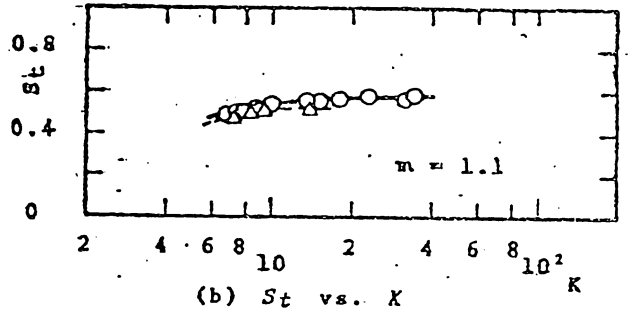
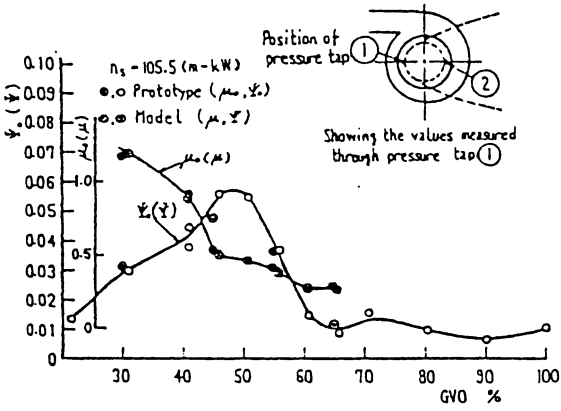


Fig. c18 Comparison of surge characteristics in the present draft tube with those in the model turbine

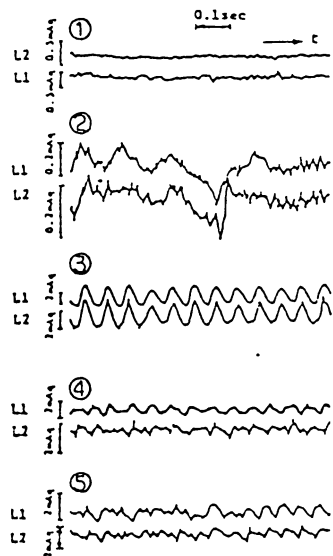
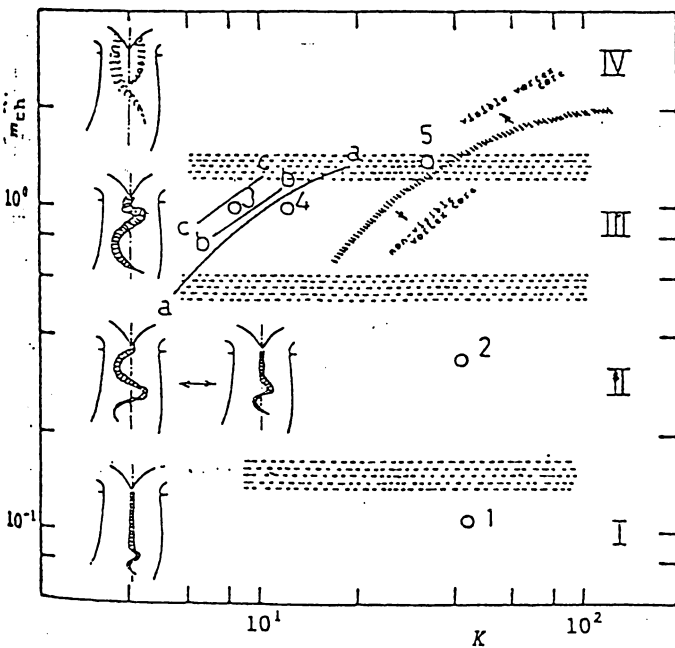


Fig. c20 Examples of pressure fluctuation

(d) Links with hydro-elastic phenomena in the machine  
and in the system

List of Papers

- (d1) Shoji, H. and Ohashi, H, "Analytical Study of Fluid Forces on Whirling Centrifugal Impeller in Vaneless Diffuser", Trans. JSME, Vol. 47, No. 419, July 1981, pp. 1187-1196, (in Japanese).  
"Fluid Forces on Rotating Centrifugal Impeller with Whirling Motion", NASA Conference Publication 2133, 1980, by the same authors is equivalent English version.
- (d2) Ohashi, H. et al, "Experimental Study of Fluid Forces on Whirling Centrifugal Impeller in Vaneless Diffuser", ASME, Proc. Fluid Structure Interactions in Turbomachinery, Nov. 1981, Wash. D.C., p. 57-62.
- (d3) Tsujimoto, Y. et al, "Analysis of Unsteady Torque on a Centrifugal Impeller", Trans. JSME, Vol. 47, No. 418, June 1981, pp. 957-965, (in Japanese).  
"An Analysis of Unsteady Torque on a Two-Dimensional Radial Impeller" J. Fluids Eng., Vol. 104, No. 2, June 1982, pp. 228-234 by Imaichi, K. et al is equivalent English version.
- (d4) Tsujimoto, Y. et al, "Analysis of Unsteady Torque on a Quasi-Three Dimensional Impeller", to be published in Trans. JSME, Vol. 50, No. 450, Feb. 1984, (in Japanese).
- (d5) Tsujimoto, Y. et al, "Analysis of Unsteady Torque on a Mixed-Flow Impeller", JSME, Preprint 834-7, March 1983, p. 45-48, (in Japanese).
- (d6) Kanki, H., Kawata, Y. and Kawakami, T., "Experimental Research on the Hydraulic Excitation Force on the Pump Shaft", ASME Paper 81-DET-71, Sept. 1981.
- (d7) Okamura, T., "Radial Thrust in Centrifugal Pumps with Single-Vane Impeller", Bulletin JSME, Vol. 23, No. 180, June 1980, pp. 895-901.
- (d8) Aoki, M., "Instantaneous Pressure Distributions Between Blades and Fluctuating Thrust in the Single Blade Centrifugal Pump", Turbomachinery Society of Japan, Conf. Preprint, Oct. 1982, (in Japanese).
- (d9) Yamaguchi, Y. and Miura, S., "Characteristics of Radial Force Fluctuations on Runners of Francis-Type Pump-Turbines. 1st Rep., Experiments on General Characteristics of Radial Force Fluctuations and Effects of Structural Factors.", Bulletin JSME, Vol. 24, No. 195, Sept. 1981, pp. 1586-1593.

- (d10) Yamaguchi, Y. and Ito, H., "Experimental Research on Stress Fluctuations in Runner Vanes of High-Head Pump-Turbines", Bulletin JSME, Vol. 24, No. 195, Sept. 1981, pp. 1594-1601.
- (d11) Nagafuji, T. and Sugishita, K., "Dynamic Measurement of Pressure Field Around the Runner of Pump-Turbines", Turbomachinery, Vol. 11, No. 3, March 1983, pp. 157-163, (in Japanese).
- (d12) Kubota, N. and Uranishi, K., "Axial-Thrust Fluctuations of a Pump with Low Specific Speed", JSME, Preprint 820-10, Sept. 1982, pp. 110-112, (in Japanese).

### Summary

Papers d1 to d5 are concerned with rotor dynamic problems of bending and torsional mode.

Paper d1 deals with the analysis of fluiddynamic lateral forces on a centrifugal impeller, which whirls on a circular orbit in vaneless diffuser, or in other words, rotates on a flexible shaft in bending vibration. These forces are necessary to evaluate the response of the rotor system to external excitation or to judge the stability of the rotor system at a specific rotational speed. The paper d1 solved the unsteady flow around whirling impeller, assuming incompressible, inviscid flow, however taking account of unsteady shed vortices from impeller vanes. The result showed that the lateral force on whirling impeller acted as damping for the calculated geometry of impellers with various vane angle and number of vanes.

Paper d2 is the result of corresponding experiment. Test impellers were set into forced orbital motion and the impeller forces were measured at various flow rate and orbital to rotational freq. ratio  $\Omega/\omega$ . Fig.d1 shows typical result. Lateral force  $F$  is divided into radial and tangential components to the orbit, and each component  $F_r$  and  $F_\theta$  is normalized by

$$f_r = F_r / M\epsilon\omega^2, \quad f_\theta = F_\theta / M\epsilon\omega^2, \quad f_\theta' = F_\theta / M\epsilon\Omega\omega \quad (d1)$$

where  $M$  is mass of fluid displaced by the outer periphery of impeller,  $\epsilon$  is eccentricity,  $\Omega$  and  $\omega$  are orbital and rotational angular frequency. In the figure calculated response by paper d1 is also plotted by broken lines. These results suggest that lateral impeller force works in most condition as damping, however, may act as excitation when flow rate is near shut-off and rotational frequency is much higher than the critical frequency of the shaft.

In papers d3 to d5 analyses are given for the calculation of unsteady torque when rotational frequency and/or flow rate fluctuates sinusoidally around its mean value. Unsteady torque is divided into three parts, that is, quasi-steady, apparent-mass and wake-effect components, so that their physical meaning can be easily understood.

Among these three components, quasi-steady torque can be calculated from steady characteristics. Wake-effect torque is comparatively smaller than apparent-mass torque and the latter is calculated and given in diagrams for wide variety of impeller geometries. Fig.d2 shows as an example the phase and amplitude relation of dynamic torque to quasi-steady one for impellers with three different vane angle  $\beta$ , where  $k$  is reduced frequency and  $N$  is number of vanes. The result shows that the dynamic torque acts as damping when the impeller shaft is in torsional vibration.

Paper d3 gives the theory for a two-dimensional centrifugal impeller, while d4 for a three-dimensional centrifugal impeller using quasi-three-dimensional analysis and d5 for a mixed-flow impeller. In the latter two papers, the effect of impeller configuration on the dynamic torque was discussed.

The remaining papers d6 to d12 give information on the dynamic radial and axial thrust, pressure and stress fluctuation in pumps and turbines, when these machines operate at steady, non-vibrating condition. Paper d6 gives experimental result on dynamic radial force and on the pressure distribution around test impeller, when it rotates in double volute casing and in vaned diffuser. As shown in Fig.d3 radial thrust in double volute casing varies with the direction of shaft eccentricity and with flow rate. At low flow rate thrust fluctuation becomes much larger than its ensemble averaged value.

Single-vaned impellers are used for non-clog pumps such as sewage and slurry pumps, and have large fluctuation of radial thrust due to the strong interaction between volute and long impeller vane. Papers d7 and d8 give experimental data on the magnitude and direction of instantaneous radial thrust as function of relative location of impeller vane to volute tongue. Unsteady pressure distribution was also measured, so that the cause of large radial thrust was made clear.

In paper d9 fluctuating radial thrust on Francis-pump/turbine runners with five different specific speeds was measured during pump and turbine operation under steady and transient condition. Fig.d4 shows thrust fluctuation  $K$  relative to the value  $K_0$  at efficiency maximum point during pump operation. The result indicates clearly that the fluctuation amplitude becomes maximum at higher head and partial flow rate. Thrust fluctuation was also measured at turbine operation and during transient such as input and load rejection.

Paper d10 describes experimental data on the stress fluctuation of a model pump/turbine runner with 500 m head rise. In paper d11 unsteady pressure field around a pump/turbine runner was measured with the special emphasis how the pressure field excited the bending vibration of crown and band. A simplified model test was also conducted to check the importance of spinning pressure field caused by the interaction between vanes and wicket gates. The result suggested that only vane/gate interaction with spinning condition could cause resonance of runner vibration.

Paper d12 deals with the fluctuation of axial thrust on a centrifugal impeller. Experiment indicated that thrust fluctuation increased as flow rate decreased, and changed considerably with the configuration of diffuser and return channel.

Figures

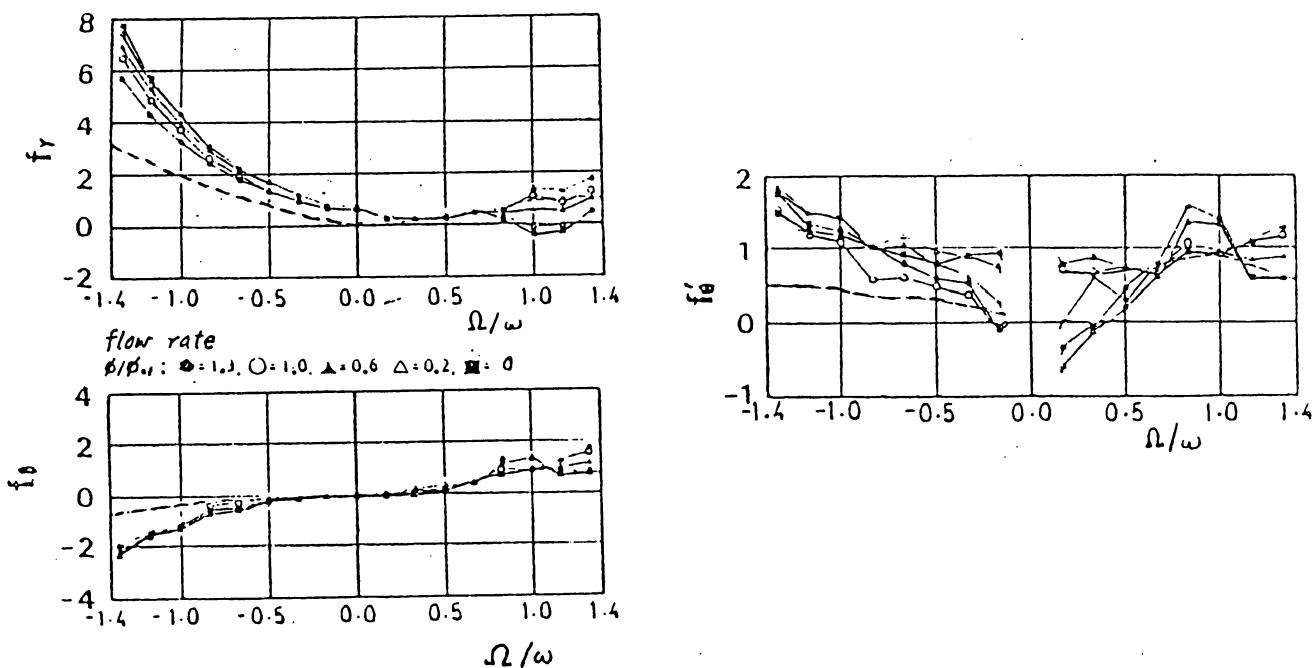


Fig.d1 Fluid forces on a whirling centrifugal impeller

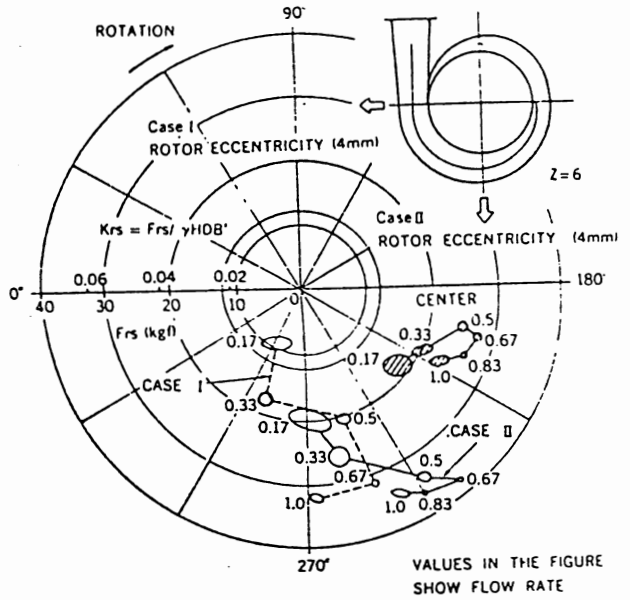
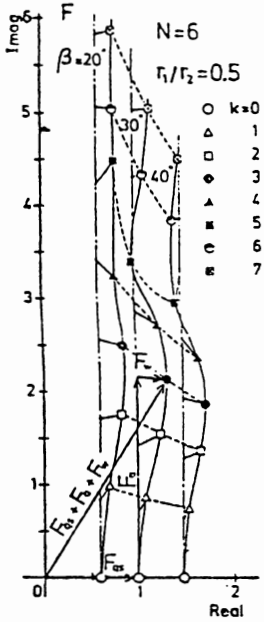


Fig.d2 Response of torque to the fluctuation of rotational frequency.

Fig.d3 Radial thrust and shaft eccentricity in double volute casing

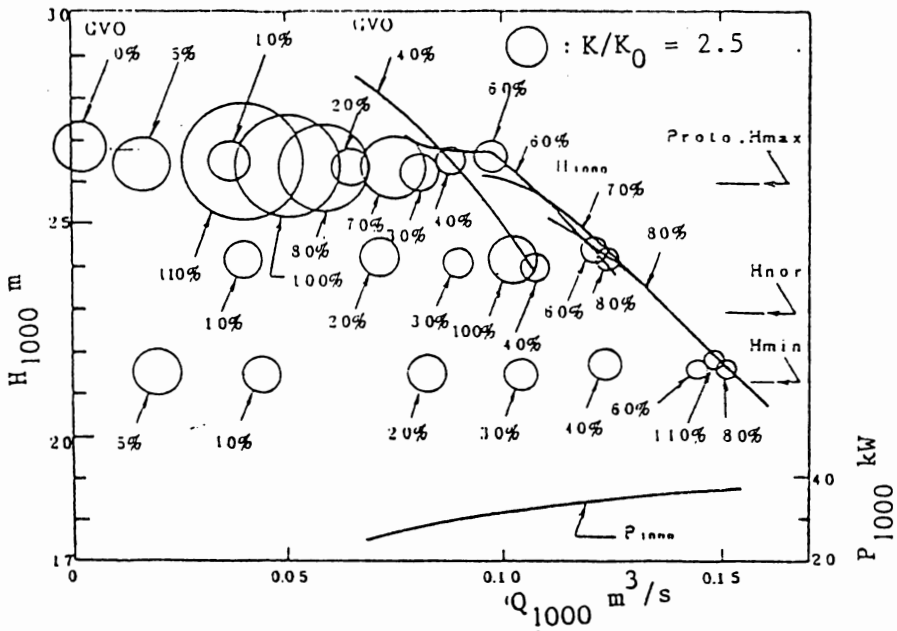


Fig.d4 Fluctuation of radial thrust of a pump/turbine runner at various operating conditions



## Conclusions

Papers written by the Japanese were summarized.

It is necessary to discuss the unsolved problems and make the research target on the basis of the state-of-the-art on the research. A special effort must be given to investigate the flow under partial load conditions of hydraulic turbines and under low flow rate conditions of pumps. Systematic and precise measurements of unsteady flow phenomena are expected.